

Research Article

Kinetic Study of Methane Hydrate Formation in the Presence of Silver Nanoparticles Synthesized by Gelcasting to Mimic Molecular Printing

Manteghian M^{1*} and Mahani AAZ²¹Chemical Engineering Faculty, Tarbiat Modares University, Iran²Chemical Engineering Department, Engineering Faculty, University of Qom, Iran***Corresponding author:** Mehrdad Manteghian, Chemical Engineering Faculty, Tarbiat Modares University, Tehran, Iran**Received:** April 17, 2022; **Accepted:** September 23, 2022; **Published:** September 30, 2022**Abstract**

Induction time of nucleation and gas storage capacity of methane hydrate in the presence of silver nanoparticles were studied. Silver nanoparticles were synthesized by gelcasting in a pre- designed polymer media. A methyl-bearing polymer was used as media in the synthesis of the nanoparticles by a reduction method. The plan provided the possibility that methyl group leaves a footprint on the silver nanoparticle after polymer decomposition. The footprint could then enhance adsorption of methane on the nanoparticles and help nucleation of methane hydrate. Induction time for nucleation was measured at initial pressures of 4.8, 5.8 and 6.8 MPa and temperatures 275.15 and 276.15 K. The conclusion was that induction time decreased dramatically in the presence of silver nanoparticles synthesized by gelcasting, and comparing the results with other works, in which silver nanoparticles synthesized with a different method was used, revealed that the method of synthesis and the footprints could be important parameters.

Keywords: Methane hydrate; Induction time, Silver nanoparticles; Gelcasting

Nomenclature

A_i, B_i, C_i : Langmuir Constant; f : Fugacity; M : Hydration number; n : Number of moles; V_{w_0} : Moles of water at initial state; N_A : Avogadro constant; P : Pressure; R : Universal gas constant; SC : Storage capacity; T_{ind} : Induction time; V_t : Volume of gas at time t ; V_{cell} : Hydrate reactor volume; V_{s_0} : Volume of solution at initial state; V_{RWT} : Volume of reacted water at time t ; V_{Ht} : Volume of formed hydrate at time t ; V_{STP} : Volume of gas at standard temperature and pressure; v_w^{MT} : Molar volume of hydrate; v_w^L : Molar volume of water; Z : Compressibility factor; Δn_{CH_4} : Mole of consumed methane; θ_i : Fractional occupancy

Introduction

Gas hydrates are receiving interest as a storage cradle for natural gas [1]. There are some problems in its industrialization, with long formation time mentioned as one. Many researchers have worked on the promotion of kinetics of methane hydrate formation using surfactants [1-4]. Using nanoparticles has recently attracted the attention of researchers as a kinetic promoter of hydrate [5,6]. Arjang et al [7] used silver nanoparticles synthesized by a reduction method and it was concluded that methane hydrate induction time decreased by 85% and 74% for the experiments started with pressures of 4.7 MPa and 5.7 MPa respectively.

Using silver nanoparticles and SDS for promotion of CO₂ hydrate formation have been reported by Mohammadi et al [8]. Since the induction time of CO₂ hydrate with pure water was short, Ag and SDS didn't have a significant effect on the induction time. Ag and SDS didn't improve storage capacity when used separately, but their co-presence had a significant effect on increasing gas storage capacity.

Govindaraj et al investigated the effect of nano-silica and activated

carbon on methane hydrate formation [9]. Chari et al [10] surveyed the effect of nanoparticles of silica on formation and dissociation of methane hydrate and they have reported that the yield of hydrate formation reached 45% while the yield from pure water was 2.4%.

Silver has a high heat conductivity coefficient and can improve the conductivity of water and consequently heat removal from the mixture during the hydrate formation could be done with a higher rate as compared to pure water. In the present work, silver nanoparticles were synthesized using the gelcasting method. Gelcasting method and its procedure has been explained elsewhere [11]. It's supposed that nanoparticles, synthesized by gelcasting with a polymer that contains methyl group, could exhibit molecular imprinting of this CH₃ structure (Figure 1). This effect of the nanoparticles can improve the adsorption and solubility of methane in water.

Experiments**Material**

Table 1 shows the materials used in this study along with their suppliers and purity. All chemicals were used as they purchased from the manufacturer. Deionized water was used for preparing all solution samples. Aqueous solutions were prepared using an accurate analytical balance with an uncertainty of ± 0.1 mg

Apparatus

A schematic diagram of the experimental set up used in the present work is shown in (Figure 2). The hydrate cell is made from stainless steel with an inside volume of 460 cm³ and has a jacket for cooling. There are three valves for introducing the gas and solution, discharging the mixture and washing the cell. A Lauda

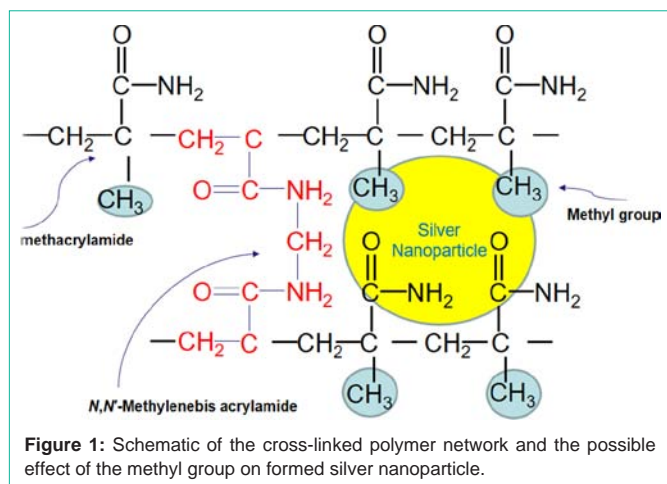
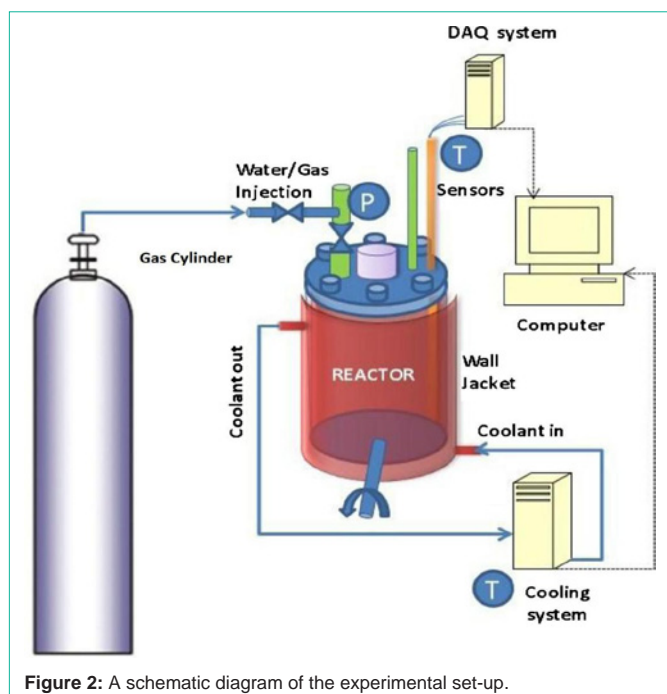


Table 1: Purities and suppliers of the chemicals used in this study.

Chemical	Supplier	Purity
Methacrylamide	Merck	99.0 (wt%)
N,N'-methylene bis acrylamide	Merck	98.0 (wt%)
N,N,N',N'-tetramethyl ethylene diamine	Merck	98.0 (wt%)
Ammonium persulfate	Merck	98.0 (wt%)
Trisodium citrate	Merck	99.0 (wt%)
Silver nitrate	Simab Co.	99.0 (wt%)
Methane	Technical gas services	99.99% (Mole%)



cooling circulator is connected to the jacket of the cell to adjust the temperature of the cell. The cell and coolant tubes are insulated. A pressure and a temperature indicator, used for measuring the temperature and pressure of the cell inside are connected to a data acquisition system. The cell is connected to an electromotor via the

connector for mixing the gas and solution with a rocking movement.

Procedure

To determine the induction time for hydrate nucleation these steps were followed. Before each experiment, the cell was washed with water and dried and evacuated by the vacuum pump. After loading the cell with 100 ml of water or nanofluid (a mixture of water and nanoparticles) the cell temperature was adjusted either to 275.15 or 276.25 K. After reaching the desired temperature data recording was started and gas was loaded to the cell to initial pressures of 4.8, 5.8 or 6.8 MP by a high pressurized gas cylinder. Finally, the electrometer was started to begin mixing. For storage capacity measurement and water to hydrate conversion tests, 25 ml of solution or pure water was injected into the cell; other steps were the same as induction time tests.

Synthesis of Silver Nanoparticles and Nanofluid Suspension

In the present work, silver nanoparticles were synthesized by decomposition of AgNO_3 via gelcasting. Initially, the methacrylamide (4.250 g) and N, N'-methylene bis acrylamide (0.425 g) were added to 20g water, and then silver nitrate (0.280 g) was added to the solution. A magnetic stirrer was used for homogenizing the solution. APS solution and TEMED were added to the solution as initiator and catalyst, respectively. Then, the solution was stirred until the gel formed. For the accomplishment of the gelcasting process, the gel should be calcined at high temperatures; therefore the sample was heated in the furnace at 650°C for 6 hours. After calcination, the silver powder was obtained. The powder was washed with water for removing any impurities. Figure 3 shows the SEM image of the synthesized silver nanoparticles.

A reference solution was made by dispersing the obtained powder in the presence of trisodium citrate using an ultrasonic homogenizer. For each hydrate formation experiment, a specified amount of this solution was introduced to a 100 ml vessel and the final aqueous solution was prepared by adding deionized water.

Formula

The amount of consumed gas was calculated based on the real gas law by Equation 1. Where P, T, V are pressure, temperature and volume of the gas. Z, the compressibility factor is calculated by the

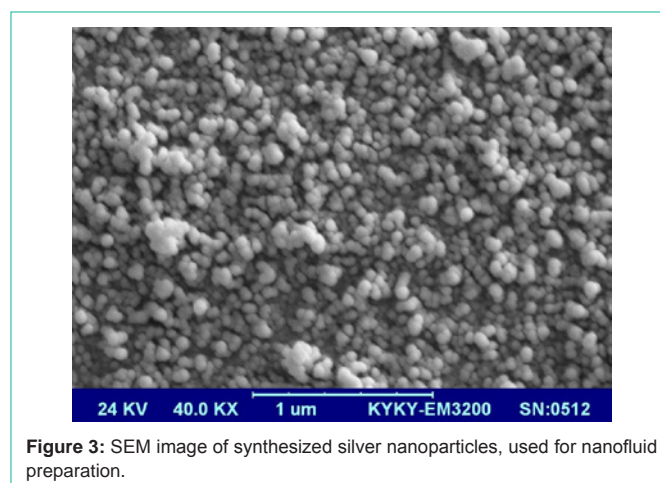


Table 2: Langmuir constant for Equation 10 [13].

Gas	Structure	Small Cavity (S)		Large Cavity (L)	
		$A_i \times 1000(k/arm)$	$B_i(K)$	$A_i \times 1000(k/arm)$	$B_i(K)$
CH_4	I	0.7228	3187	23.35	2653

PRSV (Peng–Robinson–Stryjek–Vera) Equation of state and R is the gas constant. Indices of 0 and t are related to the value of the parameter at the time $t=0$ and $t=t$ respectively. V_i is calculated by Equation 2.

$$\Delta n_{CH_4} = \frac{P_0 V_0}{Z_0 R T_0} - \frac{P_t V_t}{Z_t R T_t} \quad (1)$$

$$V_t = V_{cell} - V_{s_0} + V_{RW_t} - V_{H_t} \quad (2)$$

V_{cell} is the volume inside the cell, V_{s_0} is the initial solution volume, V_{RW_t} is the volume of the reacted water at time t and V_{H_t} is the volume of the formed hydrate at time t.

Considering the physical reaction 3 between water and methane one can assume that by consumption of mol of methane mol of water has reacted. V_{RW_t} and V_{H_t} are calculated by Equations 4 and 5. Since methane hydrate in pure water form structure I of hydrate so the molar volume of water and hydrate are calculated by Equations 6 [8] and 7 [12].



$$CH_4 \times V_{RW_t} = M \times \Delta n_{CH_4} \times v_w^L \quad (4)$$

$$V_{RW_t} = M \times \Delta n_{CH_4} \times v_w^L \quad (5)$$

$$v_w^L = 8.015 \times [1 - (1.001 \times 10^{-2}) + (1.33391 \times 10^{-4})[1.8(T - 273.15) + 32] + (5.50654 \times 10^{-7})[1.8(T - 273.15) + 32]^2] \times 10^{-3} \quad (6)$$

$$v_w^{MT} [1] = (11.835 + 2.217 \times 10^{-5} T + 2.242 \times 10^{-6} T^2)^3 \frac{10^{-30} N_A}{46} - 8.006 \times 10^{-9} P + 5.448 \times 10^{-12} P^2 \quad (7)$$

M is hydration number and depends on the fraction of large or small cage of hydrate occupied by methane molecules and calculated by Equation 8. And are the fractional occupancy of large (L) and small (S) cavities, respectively, and are calculated based on Langmuir adsorption theory, Equation 9. C_i is the Langmuir constant of methane for cavity type i; f_{CH_4} represents the fugacity of methane in the gas phase.

$$M = \frac{46}{6\theta_L + 2\theta_S} \quad (8)$$

$$\theta_i = \frac{C_i f_{CH_4}}{6\theta_L + 2\theta_S} \quad (9)$$

C_i is calculated by Equation 10. Where T is the temperature, A_i and B_i are constants. Table 2 shows the values of A_i and B_i for small and large cavities [13].

$$Conversion = \frac{M X \Delta n_{CH_4}}{n W_0} \quad (13)$$

$$C_i = \frac{A_i}{T} \exp\left(\frac{B_i}{T}\right) \quad (10)$$

For a specific gas, M is a function of temperature and fugacity so in the present work we assume M as a constant parameter and it was calculated by averaging M over the highest and the lowest fugacity. By using already discussed calculation and averaging the M consider 5.98.

By replacing from Equations 4 and 5 into Equation 1, can be calculated by Equation 11.

$$\Delta n_{CH_4} = \frac{\frac{P_0 V_0}{Z_0 R T_0} - \frac{P_t (V_{cell} - V_{s_0})}{Z_t R T_t}}{\left(1 + \frac{P M (v_w^L - v_w^{MT})}{Z_t R T_t}\right)} \quad (11)$$

This calculation method does not need trial and error as other researchers have used [14,15].

The gas storage capacity can be defined as the utmost volume of gas at the standard condition that can be trapped in the hydrate crystal. Gas storage capacity is calculated by Equation 12, in which the TSTP is the standard temperature (273.15 K) and PSTP is the standard pressure (101325 Pa). Δn_{CH_4} is the total consumed gas at the end of the hydrate formation process and V_H is the total volume of water converted to hydrate.

$$SC = \frac{V_{STP}}{V_H} = \frac{\Delta n_{CH_4} R T_{STP} / P_{STP}}{V_H} \quad (12)$$

Water to hydrate conversion is calculated by Equation 13.

Experimental Design

The initial pressure at 3 levels of 4.8, 5.8 and 6.8 Mpa, the temperature at 2 levels of 275.15 and

276.15 K and nanofluid concentration at 4 levels of 6.25, 12.5, 18.75 and 25 ppm were surveyed. One experiment was done with 250 ppm trisodium citrate at 4.8 Mpa and 275.15 K for determining its effect on the induction time. Storage capacity tests were done in the presence of 12.5, 25, 37.5 and 50 ppm nanofluid. For simplicity, we only mention the concentration of silver nanoparticles. It is evident that in each nanofluid sample a specific amount of trisodium citrate exists to act as a stabilizer.

Results and Discussion

Gas Hydrate Induction Time

Table 3 shows the induction times and gas consumption 100 min after nucleation time for different initial temperatures and pressures. In this work, induction time was measured from the injection point until a sudden decrease in pressure (hydrate formation). Hydrate formation is confirmed by a sudden increase in temperature inside the cell. Figures 4 and 5 show the pressure and temperature variations in experiments 1 and 2. As shown in these figures the pressure reduction was rapid at first because of the gas cooling and dissolution in water

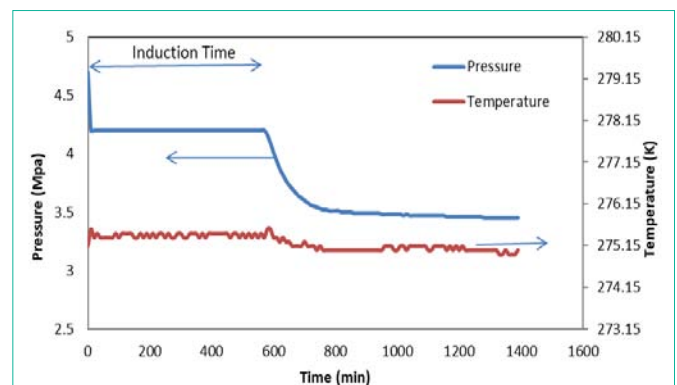


Figure 4: Pressure and temperature variations during hydrate formation from pure water at initial pressure 4.8 MPa, temperature 275.15 K.

Table 3: Induction time and gas consumption.

Exp.	Initial pressure (MPa)	Temperature (K)	Sample Concentration (ppm)	Induction time (min)	Gas consumption 100 min after inductiontime (mol)
1	4.8	275.15	0	570	0.2012
2	4.8	275.15	6.25	21	0.2335
3	4.8	275.15	12.5	13	0.2164
4	4.8	275.15	18.75	13	0.2414
5	4.8	275.15	25	8	0.2084
6	4.8	275.15	250 ppm Trisodium citrate	510	0.1921
7	4.8	276.15	0	Not Formed	N/A
8	4.8	276.15	6.25	Not Formed	N/A
9	4.8	276.15	12.5	1170	0.2043
10	4.8	276.15	18.75	615	0.2107
11	4.8	276.15	25	19	0.2059
12	5.8	275.15	0	290	0.2147
13	5.8	275.15	6.25	12	0.2653
14	5.8	275.15	12.5	7	0.2347
15	5.8	275.15	18.75	5	0.1938
16	5.8	275.15	25	2	0.2411
17	5.8	276.15	0	Not Formed	N/A
18	5.8	276.15	6.25	1458	0.2455
19	5.8	276.15	12.5	1185	0.2346
20	5.8	276.15	18.75	170	0.2417
21	5.8	276.15	25	22	0.2233
22	6.8	275.15	0	8	0.3219
23	6.8	275.15	6.25	1.5	0.2705
24	6.8	275.15	12.5	1	0.3239
25	6.8	275.15	18.75	0.5	0.2598
26	6.8	275.15	25	0.5	0.3146
27	6.8	276.15	0	8	0.2765
28	6.8	276.15	6.25	14	0.3524
29	6.8	276.15	12.5	4	0.2915
30	6.8	276.15	18.75	2	0.2407
31	6.8	276.15	25	0.5	0.3177

and then the pressure remained constant. This period is related to nucleation, during which the nuclei form and growth begins until a critical size is reached. The induction time of pure water and 6.25 ppm Ag nanofluid as shown in the figures at initial condition of P=4.8 MPa and T=275.15 K were 570 and 21 min respectively. After this period a sudden reduction in pressure is observed owing to hydrate growth.

Figure 6 illustrates the induction time of methane hydrate in the presence of different nanofluids. A general decrease in the induction time is evident as the concentration of silver nanoparticles increases. In the experiment with the initial pressure of 4.8 Mpa and temperature of 275.15 K the induction time was 570 min but in the presence of

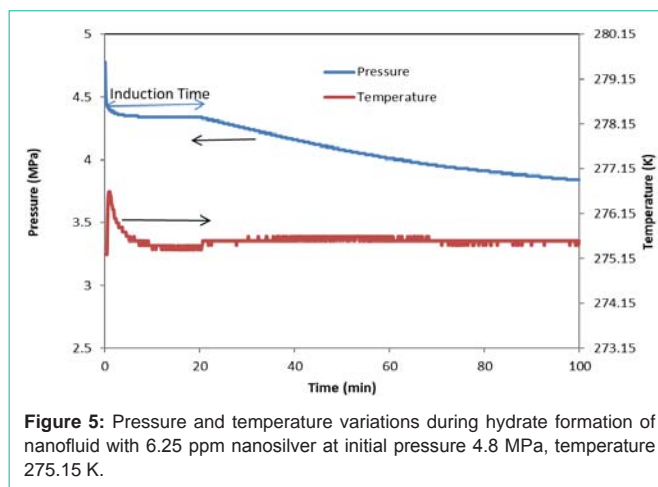


Figure 5: Pressure and temperature variations during hydrate formation of nanofluid with 6.25 ppm nanosilver at initial pressure 4.8 MPa, temperature 275.15 K.

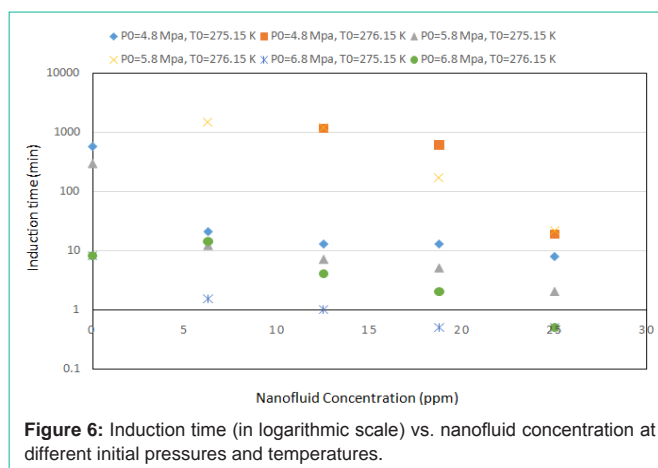


Figure 6: Induction time (in logarithmic scale) vs. nanofluid concentration at different initial pressures and temperatures.

25 ppm nanoparticles, the induction time decreased to 8 min. With this nanofluid 98.5 percent reduction in induction time was achieved. It is evident from Table 2 that the induction time decreased when nanoparticle concentration increased.

In the experiments with initial condition of P=4.8 Mpa and T=276.15 K, when the cell was loaded with pure water no hydrate formed, due to low super saturation and high induction time. The addition of nanoparticles with a concentration of 6.25 ppm did not result in any hydrate formation. But with a nanofluid concentration of 25ppm hydrate formed and the induction time was 19 min indicating that the nanofluid has caused a substantial decrease in the induction time and nucleation took place even at this low super saturation.

In the experiments with initial pressure of 5.8 MPa and temperature 275.15 K reduction of the induction time from 290 min for pure water to 2 min for 25 ppm nanofluid can be seen. Nanoparticle concentration had a great effect on the induction time. With 6.25 ppm Ag, the induction time was about 12 min. The hydrate of pure water did not form with an initial pressure of 5.8 MPa and a set temperature of 276.15. In the presence of 6.25 ppm Ag, the induction time was 1458 min and it reached 2 min with 25 ppm Ag.

In experiments with an initial pressure of 6.8 MPa induction times were considerably lower than when initial pressures were 4.8 and 5.8 MPa, because of higher super saturation. The hydrate of pure

Table 4: Induction time in the presence of silver nanoparticles synthesized by different methods at initial temperature 275.15K.

Nanosilver synthesized by inverse microemulsion method [16]				Triangular nanosilver synthesized by reduction method [17]				Nanosilver synthesized by gelcasting method (present study)			
Initial pressure (MPa)	Nanofluid Concentration (ppm)	Induction time (min)	Induction time reduction (%)	Initial pressure (MPa)	Nanofluid Concentration (ppm)	Induction time (min)	Induction time reduction (%)	Initial pressure (MPa)	Nanofluid Concentration (ppm)	Induction time (min)	Induction time reduction (%)
5.7	0	380.3	0	5.5	0	222.7	0	5.8	0	290	0
5.7	0.535	220.8	41.9	5.5	0.855	9.3	95.8	5.8	6.25	12	95.9
5.7	1.337	133.7	64.8	5.5	1.550	7	96.8	5.8	12.5	7	97.6
5.7	2.675	68.2	82.1	5.5	3.120	14.4	93.5	5.8	18.75	5	98.3
5.7	5.35	99.2	73.9	5.5	4.670	22	90.1	5.8	25	2	99.3
5.7	10.7	145.8	61.6	5.5	6.24	29	86.9	-	-	-	-
5.7	16.05	190	50	-	-	-	-	-	-	-	-

Table 5: Induction time in the presence of silver nanoparticles synthesized by different methods at initial temperature 275.15K.

Nanosilver synthesized by inverse microemulsion method [16]				Triangular nanosilver synthesized by reduction method [17]				Nanosilver synthesized by gelcasting method (present study)			
Initial pressure (MPa)	Nanofluid Concentration (ppm)	Induction time (min)	Induction time reduction (%)	Initial pressure (MPa)	Nanofluid Concentration (ppm)	Induction time (min)	Induction time reduction (%)	Initial pressure (MPa)	Nanofluid Concentration (ppm)	Induction time (min)	Induction time reduction (%)
4.7	0	485	0	4.7	0	402	0	4.8	0	570	0
4.7	0.535	263.8	45.6	4.7	0.855	39.4	90.2	4.8	6.25	21	96.3
4.7	1.337	242.5	50	4.7	1.550	21.5	94.6	4.8	12.5	13	97.7
4.7	2.675	129.3	73.3	4.7	3.120	12.2	96.9	4.8	18.75	13	97.7
4.7	5.35	71.4	85.3	4.7	4.670	14	96.5	4.8	25	8	98.6
4.7	10.7	116.5	80	4.7	6.24	21.7	94.6	-	-	-	-
4.7	16.05	194.2	60	-	-	-	-	-	-	-	-

water was formed in 8 min after gas injection with initial condition of P=6.8 Mpa and T=275.15 K.

With everything else remained similar, the induction time dropped to 30 seconds when the nanoparticle concentration increased to 25 ppm.

Silver as a high conductivity metal increases the conductivity and convection coefficient of nanofluid so heat removal from the nanofluid during nucleation and growth could be done more effectively rather than when pure water is used. Also, the free Gibbs energy needed for heterogeneous nucleation is less than homogeneous nucleation so nucleation in the presence of nanoparticles would be faster.

The existence of nanoparticles in the interface of water/gas improves the gas adsorption and since the nanoparticles are molecularly imprinted by the methyl group, had a large capacity for adsorption of methane and transfer them inside the liquid phase. Also, particles in the solution adsorb dissolved methane on their surfaces and facilitate the condition for forming nuclei around the particle and also these particles make the role of methane donor inside the solution.

Tables 4 and 5 contain the induction time of methane hydrate in the presence of silver nanoparticles synthesized by three different methods. A comparison between these data reveals that nanoparticles synthesized by the gelcasting method improve induction time more than the other silver nanoparticles which synthesized with reverse microemulsion [16] and reduction method [17]. So this promotion might be because of methyl group printing on the surface of nanoparticle.

Amount of Consumed Gas

Figure 7 shows the variation of the amount of consumed gas with time for the experiments performed with initial pressure of 4.8 MPa and temperature 275.15 K. The amount of consumed gas has been high just after injection time due to dissolution of gas and then it remained constant for a while that is during induction time. Again gas consumption raises just after growth starts.

Also, the gas consumption 100 min after induction time is shown in Table 2. In pure water 0.201 mol of methane was consumed 100 min after induction time, but for nanofluid of 18.75 ppm 20% increase happened and this is the best promotion at this initial condition.

Figure 8 shows the amount of consumed gas in the experiments with initial conditions of P=4.8 Mpa and T=276.15. As was

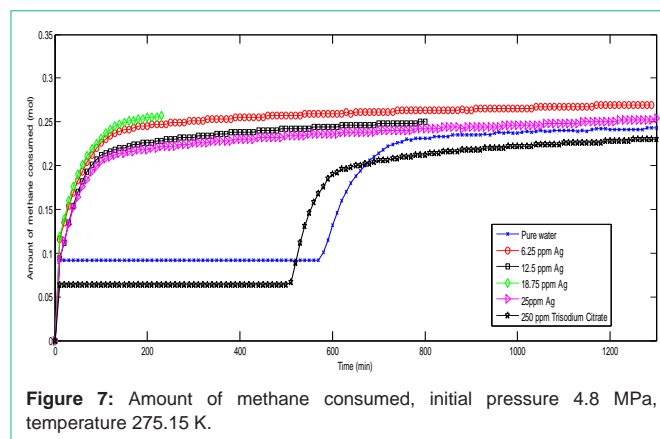


Figure 7: Amount of methane consumed, initial pressure 4.8 MPa, temperature 275.15 K.

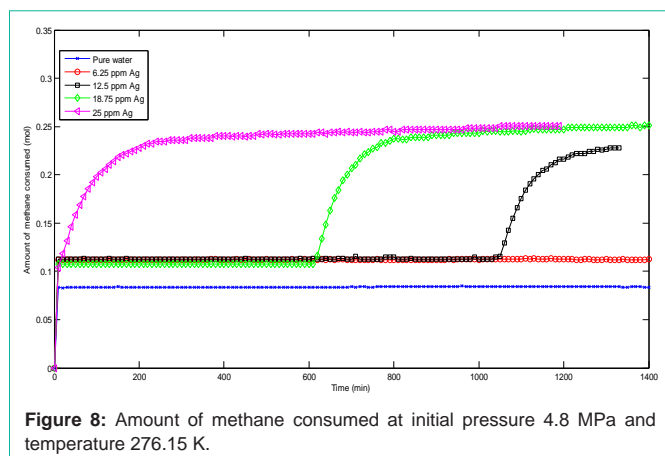


Figure 8: Amount of methane consumed at initial pressure 4.8 MPa and temperature 276.15 K.

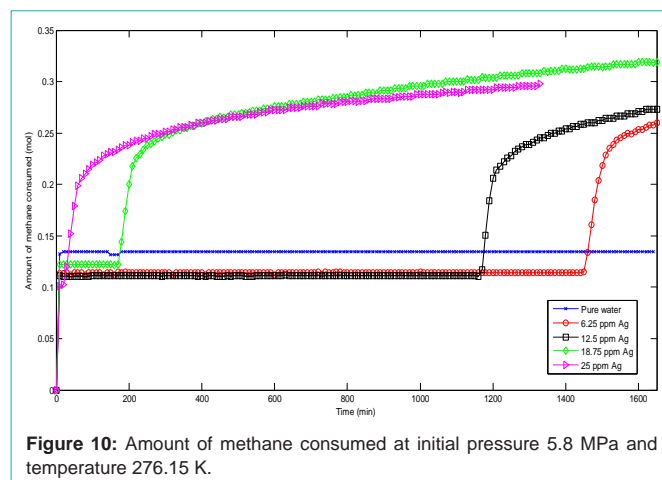


Figure 10: Amount of methane consumed at initial pressure 5.8 MPa and temperature 276.15 K.

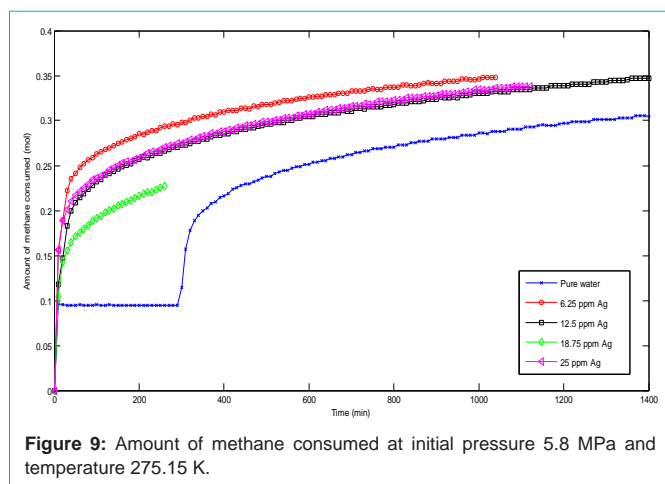


Figure 9: Amount of methane consumed at initial pressure 5.8 MPa and temperature 275.15 K.

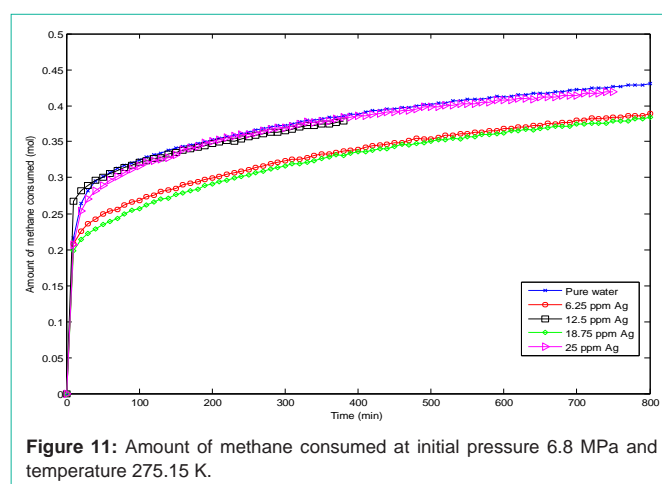


Figure 11: Amount of methane consumed at initial pressure 6.8 MPa and temperature 275.15 K.

mentioned in Table 2 the hydrate of pure water and 6.25 ppm nanofluid didn't form so the gas consumption measurement 100 min after induction time was not possible for those samples. Comparing the gas consumption for the other concentration shows no significant variation with concentration. But 18.75 ppm had the most gas consumption 100 min after induction time and was 0.2107 mol.

Gas consumption of experiments at $P=5.8$ MPa and $T=275.15$ K is illustrated in Figure 9. Nanofluid with 6.25 ppm Ag concentration had the most improvement in gas consumption and it was 0.2653 mol that showed 24 percent improvement compared to pure water. This concentration also was the optimum concentration for experiments of $P=5.8$ MPa and $T=276.15$ K and gas consumption 100 min after induction time was 0.2455 mol. Figure 10 shows the gas consumption of experiments at initial conditions of $P=5.8$ MPa and $T=276.15$ K.

Figure 11 shows the gas consumption of experiments at $P=6.8$ MPa and $T=275.15$ K. No improvements were seen in the presence of nanofluid. Since the supersaturation was high in this temperature and pressure, the solubility of methane in water is high, so the role of nanoparticles in increasing the absorption and solubility was neutralized. It seems that at the high supersaturation condition a big driving force between gas, dissolve gas and gas in hydrate have existed, so after growth starting a thick layer of hydrate was formed at the interface of the water/gas rapidly and this layer slowed the mass transfer from gas phase to the water [5] also it prevented the

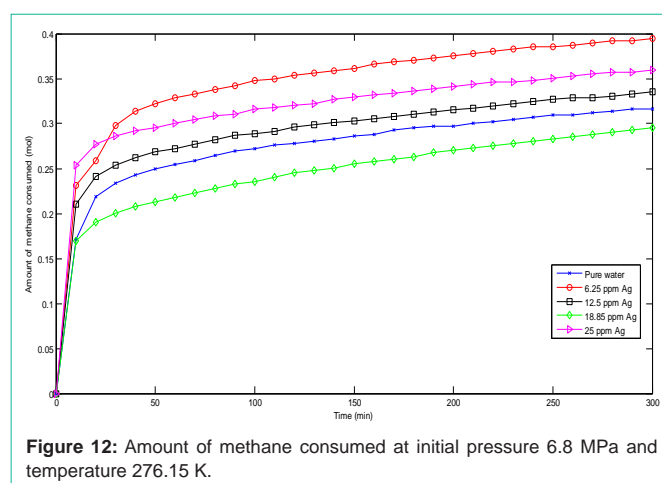


Figure 12: Amount of methane consumed at initial pressure 6.8 MPa and temperature 276.15 K.

nanoparticles existence in the water surface and adsorption of gas molecules.

Figure 12 shows the gas consumption of experiments at $P=6.8$ MPa and $T=276.15$ K. The gas consumption of pure water was 0.2765 mol, which was increased to 0.3524 mol in the presence of 6.25 ppm Ag. Nanofluid with 6.25 ppm Ag increases the gas consumption 27 percent which is considerable.

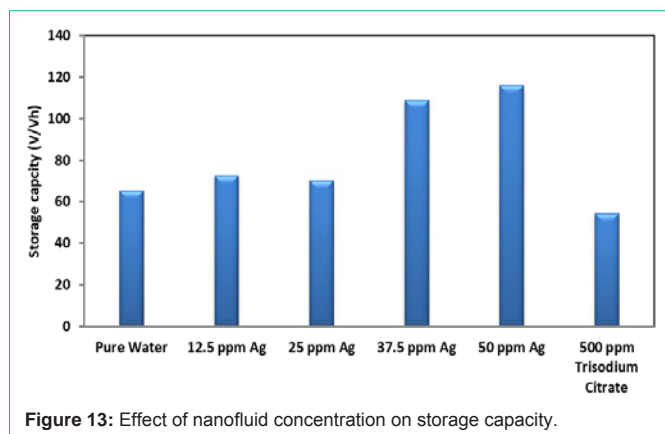


Figure 13: Effect of nanofluid concentration on storage capacity.

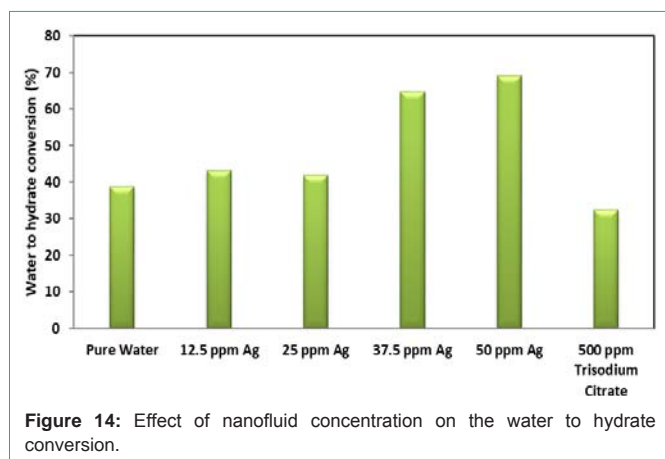


Figure 14: Effect of nanofluid concentration on the water to hydrate conversion.

Gas Storage Capacity and Water to Hydrate Conversion

The gas storage capacity of the hydrate made in the presence and absence of nanoparticles is shown in Figure 13. With pure water, the storage capacity is measured about 65 V/V and with 12.5 ppm and 25 ppm nanofluid the storage jumps to 72 and 70 V/V. Higher effects are seen at larger concentrations of nanoparticles. This is partly, perhaps, because of the offsetting effect of trisodium citrate in the nanofluid. It is shown in the figure that the presence of trisodium citrate reduces the hydrate storage capacity for methane. A 500 ppm trisodium citrate solution reduces the storage capacity to 54 V/V. Other researchers have also observed that the presence of ions in water reduces the solubility of methane in water [18,19]. So when lower concentrations of nanofluid have been applied, the positive effect of marked nanoparticles could have been challenged by the negative effect of sodium and citrate ions. Higher concentrations of nanoparticles (37.5 and 50 ppm) results in a significant promotion on the storage capacity. Nanofluid of 37.5 and 50 ppm Ag increased the storage capacity to 108 and 116 V/V, showing jumps of 67 and 78 percent compared to the gas storage capacity of the hydrate made from pure water, respectively.

Water to hydrate conversion of solutions is shown in Figure 14. Pure water conversion was measured 38.8%, while for 12.5 and 25 ppm solutions, the conversion increases to 43.1 and 41.8% respectively. Same as the storage capacity, in these two concentrations, the significant increase didn't happen. In the presence of 37.5 and 50

ppm Ag the conversion was increased to 64.7 and 69.1 %.

Water to hydrate conversion for 500 ppm trisodium citrate solution was 32.4% and was less than pure water conversion. The presence of nanoparticles and their motion in the solution led to colliding with gas bubbles that caused to break the methane bubbles [20] and made them smaller, so the smaller bubbles increase the area to volume ratio and consequently increase the mass transfer rate. The inhibition effect of trisodium citrate could be because of presence of sodium and citrate ions inside the solution so these ions existence decreased the solubility of methane inside the solution.

Conclusion

In this work, the effect of silver nanoparticles synthesized by the gelcasting method on induction time and gas storage capacity of methane hydrate was studied. The presence of silver nanoparticles promotes the formation of methane hydrate. The nanofluid contained silver nanoparticles reduced the induction time up to 98%. Also the comparison with the results of the presence of silver nanoparticles which synthesized by reduction and microemulsion method revealed that the method of synthesis is an important factor in the effectiveness of the nanoparticles. Silver nanoparticles synthesized by gelcasting could be molecularly imprinted by methyl group existing on the polymer used to stabilize nanoparticles during synthesis and these phenomena improve the effectiveness of the nanoparticles in absorbing the methane. The storage capacity of hydrate in the presence of 37.5 and 50 ppm Ag nanoparticles increased 67 and 78% respectively.

Nanoparticles and trisodium citrate in the solution have positive and negative effects on induction time and storage capacity of pure water and these non-consistent effects are in the challenge and their resultant determine promotion or inhibition.

References

1. Ganji H, Manteghian M, Sadaghianzadeh K, Omidkhan MR, Rahimi Mofrad H. Effect of different surfactants on methane hydrate formation rate, stability and storage capacity. *Fuel*. 2007; 86: 434-441.
2. Ganji H, Manteghian M, Mofrad HR. Effect of mixed compounds on methane hydrate formation and dissociation rates and storage capacity. *Fuel Processing Technology* 2007; 88: 891-895.
3. Lin W, Chen G-J, Sun C-Y, Guo X-Q, Z.-K.Wu, Liang M-Y, et al. Effect of surfactant on the formation and dissociation kinetic behavior of methane hydrate. *Chemical Engineering Science*. 2004; 59: 4449-4455.
4. Zhang CS, Fan SS, Liang DQ, Guo KH. Effect of additives on formation of natural gas hydrate. *Fuel*. 2004; 83: 2115-2121.
5. Park S-S, An E-J, Lee S-B, Chun W-g, Kim N-J. Characteristics of methane hydrate formation in carbon nanofluid. *Journal of Industrial and Engineering Chemistry*. 2012; 18: 443-448.
6. Li J, Liang D, Guo K, Wang R, Fan S. Formation and dissociation of HFC134a gas hydrate in nano-copper suspension. *Energy Conversion and Management*. 2006; 47: 201-210.
7. Arjang S, Manteghian M, Mohammadi A. Effect of synthesized silver nanoparticles in promoting methane hydrate formation at 4.7MPa and 5.7MPa. *Chemical Engineering Research and Design*. 2013; 91: 1050-1054.
8. Mohammadi A, Manteghian M, Haghtalab A, Mohammadi AH, Rahmati-Abkenar M. Kinetic study of carbon dioxide hydrate formation in presence of silver nanoparticles and SDS. *Chemical Engineering Journal*. 2014; 237: 387-395.
9. Govindaraj V, Mech D, Pandey G, Nagarajan R, Sangwai JS. Kinetics of

- methane hydrate formation in the presence of activated carbon and nano-silica suspensions in pure water. *Journal of Natural Gas Science and Engineering*. 2015; 26: 810-818.
10. Chari VD., Sharma DVSGK, Prasad PSR, Murthy SR. Methane hydrates formation and dissociation in nano silica suspension. *Journal of Natural Gas Science and Engineering*. 2013; 11: 7-11.
 11. Mahani AAZ, Manteghian M, Pahlavanzadeh H. Synthesis of silver nanoparticles by gelcasting using a low toxic monomer and optimization of gelation time using the Taguchi method. *Particulate Science and Technology*. 2017; 35: 298-303.
 12. Klauda JB, Sandler SI. A Fugacity Model for Gas Hydrate Phase Equilibria. *Industrial and Engineering Chemistry Research*. 2000; 39: 3377-3386.
 13. Munck J, Skjold j0rgensen S. Computations of the formation of gas hydrates. *Chemical Engineering Science*. 1988; 43: 2661-2672.
 14. Mohammadi M, Haghtalab A, Fakhroueian Z. Experimental study and thermodynamic modeling of CO₂ gas hydrate formation in presence of zinc oxide nanoparticles. *Journal of Chemical Thermodynamics*. 2016; 96: 24-33.
 15. Mohammadi A, Manteghian M, Haghtalab A, Mohammadi AH, Rahmati-Abkenar M. Kinetic study of carbon dioxide hydrate formation in presence of silver nanoparticles and SDS. *Chemical Engineering Journal*. 2014; 237:387-395
 16. Arjang S. Investigation the effects of silver nanoparticles on methane hydrate formation, Master thesis, Tarbiat Modares University, Tehran, Iran; 2011.
 17. Rahmati-Abkenar M. Investigation of the effect of adding triangular silver nano particles on the rate of production of methane hydrate, Master thesis, Tarbiat Modares University, Tehran, Iran. 2012.
 18. Schumpe A. The estimation of gas solubilities in salt solutions. *Chemical Engineering Science*. 1993; 48: 153-158.
 19. Duan Z, Møller N, Greenberg J, Weare JH. The prediction of methane solubility in natural waters to high ionic strength from 0 to 250°C and from 0 to 1600 bar. *Geochimica et Cosmochimica Acta*. 1992; 56: 1451-1460.
 20. Haghtalab A, Mohammadi M, Fakhroueian Z. Absorption and solubility measurement of CO₂ in water-based ZnO and SiO₂ nanofluids. *Fluid Phase Equilibria*. 2015; 392: 33-42.